Article

Cellulose Nanocrystals versus Microcrystalline Cellulose as Reinforcement of Lignopolyurethane Matrix

Elaine C. Ramires [1,†], Jackson D. Megiatto Jr. [2], Alain Dufresne [3,*] and Elisabete Frollini [1,*]

1   Institute of Chemistry of São Carlos, Macromolecular Materials and Lignocellulosic Fibers Group, Center for Science and Technology of BioResources, University of São Paulo, 05513-970 São Paulo, Brazil; elaine_ramires@yahoo.com.br

2   Institute of Chemistry, University of Campinas (UNICAMP), POBox 6154, 13083-970 Campinas, Brazil; jdmj@unicamp.br

3   University Grenoble Alpes, CNRS, Grenoble INP, LGP2, F-38000 Grenoble, France

*   Correspondence: alain.dufresne@pagora.grenoble-inp.fr (A.D.); elisabete@iqsc.usp.br (E.F.)

†   Present address: Technology & Innovation, Suzano, Jacarei, 12340-010 São Paulo, Brazil.

check for updates

Abstract: Cellulose nanocrystals (CNC) exhibit remarkable properties such as being lightweight, renewability, nanoscale dimension, raw material availability, and a unique morphology. They have been widely used in film-forming composites, but the literature is scarce concerning bulky-composites (i.e., non-filmogenic). Microcrystalline cellulose (MCC) is widely available and has emerged as an important material for the reinforcement of composites. This investigation focuses on the preparation of non-filmogenic composites prepared from a polyurethane-type matrix, based on modified lignosulfonate and castor oil, reinforced with CNC or MCC, aiming to compare their reinforcing capacity. CNC was obtained through the acid hydrolysis of MCC. Sodium lignosulfonate was chemically modified using glutaraldehyde to increase its reactivity towards isocyanate groups in the synthesis of lignopolyurethane. The results show that adding CNC or MCC led to materials with improved impact strength, flexural properties, and storage modulus compared to pristine lignopolyurethane. With the exception of the flexural modulus, which was higher for the CNC-reinforced composite compared to the MCC-reinforced composite, all other properties were similar. The set of results indicates that CNC and MCC are promising for the reinforcement of polyurethane-type matrices. Bulky materials with good properties and prepared from high renewable raw material contents were obtained, meeting current expectations concerning sustainable development.

Keywords: Composites; cellulose nanocrystal; microcrystalline cellulose; lignopolyurethane

1. Introduction

Nanocrystals obtained from natural polysaccharides such as cellulose, starch, and chitin, are rigid nanosized particles that can be used to replace inorganic particles as reinforcement in bio-based nanocomposites [1–3]. Polysaccharide nanocrystals exhibit some advantages such as biodegradability, biocompatibility, non-toxicity, renewability, worldwide availability, easy processability, and an easy chemical, physical, and mechanical modification [2,4,5]. Conceptually, nanocomposites are multiphase materials in which at least one of the constituent phases has dimensions lower than 100 nm [6]. They can be made from a nano-reinforcement coming from biological or renewable raw materials and petroleum-derived non-bio-based polymer. Materials derived from biopolymer and synthetic nano-reinforcement also come under biocomposites. Biocomposites that are derived from plant fibers

(natural fibers) and biobased plastics are likely to be more ecofriendly, and such biocomposites are termed "green nanocomposites". Therefore, in true bio-based nanocomposites both the matrix and the nano reinforcement must be obtained from renewable resources or be biodegradable [7].

Cellulose is considered as the most abundant biomass material in nature. It consists of a high-molecular-weight homopolysaccharide that is composed of β-1,4-anhydro-D-glucopyranose [8,9]. An important characteristic of this polymer is that its monomer bears three hydroxyl groups. These groups and their hydrogen-bonding ability play an important role in crystalline packing and afford strong cohesion to the material [10,11].

Cellulose nanocrystals (CNC), which are also referred to as cellulose whiskers, can be isolated from any lignocellulosic source [10]. Acid hydrolysis of the biomass is generally implemented to obtain stable CNC aqueous suspensions. This process was first reported by Ranby [12] and Battista et al. [13], and this process was subsequently optimized [14,15]. The acid hydrolysis reaction involved in this process results in the extraction and release of crystalline cellulosic domains in the form of rod-shaped highly crystalline nanoparticles. Before undergoing acid hydrolysis under controlled conditions, the material is submitted to purification and bleaching, allowing the removal of non-cellulosic components, mainly hemicelluloses and lignin. The cross-sectional cleavage of the microfibrils in short nanocrystals results from the role of structural defects produced by the non-crystalline regions of the cellulose [16]. The hydrolysis kinetics is faster for non-crystalline regions surrounding and embedding cellulose microfibrils as compared to crystalline domains, and they are therefore disrupted, while the more resistant crystalline segments remain intact. The hydrolytic cleavage of glycosidic linkages is promoted by the penetration of the hydronium ions into non-crystalline regions. The ensuing suspension is then diluted with water to stop the reaction and is washed by successive centrifugations. Dialysis is subsequently performed to remove the residual free acid from the dispersion. The improved dispersion of the nanocrystals is implemented by a later stage of sonication. This global procedure must be adjusted depending on the nature of the substrate [10].

The use of cellulose nanocrystals as reinforcement in composites has attracted attention due to the increasing interest in developing new sustainable and environmentally friendly materials [17,18]. The resulting materials are considered especially promising when the polymeric matrix is also produced from renewable raw materials. In this study, this goal was accomplished using sodium lignosulfonate and castor oil in the synthesis of the polyurethane matrix.

Microcrystalline cellulose (MCC) is industrially produced mainly from wood and cotton [19] and has multiple applications, such as in the pharmaceutical, medical, and cosmetic areas [20]. The use of MCC as reinforcement in composites may still be considered to be scarce when compared, for example, to lignocellulosic fibers. However, in recent years the interest in using MCC in composites has increased [20–22]. Renewability, biodegradability, a large surface area, a low density, among other MCC properties, make it attractive for use in composites [20]. The main issue when using MCC, as well as CNC, in polymeric composites, lies in the fact that many polymeric matrices are nonpolar, which makes it difficult to disperse polar reinforcements like MCC and CNC. In the present study, the matrix corresponded to polyurethane, whose functional groups have polar sites, which may favor the dispersion of reinforcements such as MCC and CNC. In addition, the non-polar domains of the chemical structure of lignopolyurethane and CNC, or MCC [23], can also interact at the molecular level.

Polyurethanes are highly relevant materials in industry because of the broad variety of chemical structures that can be created between the urethane bonds. It results in different products, including elastomers, plastics, adhesives, and foams applicable in the medical, automotive, construction, and industrial fields among others [24–26]. The incorporation of lignin in polymeric materials, directly or after modification, is recognized as one of the most viable approaches for developing value-added materials [27]. The use of lignin in polyurethanes can be accomplished by direct substitution, combination with polyols, or by chemical modification. Lignin can increase the rigidity of the polymeric matrix, due to the aromatic rings and the presence of groups that can act as cross-linkers. The presence of alcoholic hydroxyl groups in lignin or lignosulfonate allows them to be used as a polyol

in the synthesis of the lignopolyurethane matrix [28,29]. Lignin has been used as a "macromonomer" in syntheses that lead to materials [26,30], but lignosulfonates, which are available practically worldwide, have been scarcely explored in the preparation of materials [31].

In the present study, lignosulfonate was chemically modified through a reaction with glutaraldehyde to increase the hydroxyl groups available to react with isocyanate groups in the reaction that leads to polyurethanes. Aiming to explore the use of CNC in non-filmogenic materials, and to compare their performance as a reinforcement with MCC, bio-based composites and nanocomposites were prepared from high contents of raw materials obtained from renewable resources. The polyurethane-type matrix was based on chemically modified sodium lignosulfonate and castor oil, a vegetable oil obtained from the seed of the castor bean, mainly composed of ricinoleic acid [31], and the reinforcement consisted of CNC or MCC.

2. Materials and Methods

2.1. Materials

Sodium lignosulfonate (LS) was provided by Lignin Products Ligno Tech Brazil Ltda (Cambará do Sul, Rio Grande do Sul, Brazil). According to the supplier, it is obtained from the sulfite pulping process of *Pinustaeda* wood with a weight average molecular weight (Mw) of approximately 6000 g·mol^{-1}, along with 5.5% of sulfur, 1.7% of magnesium, 0.2% of calcium, and 0.9% of sugars contents. Glutaraldehyde (25% in aqueous solution) was purchased from Vetec and was used without further purification. Methylene diphenyl diisocyanate (MDI) with 31.5% NCO group was donated by Bayer Material Science (São Paulo, Brazil). Castor oil (CO) with a hydroxyl index of 155 mg·g^{-1} KOH and number average molecular weight (Mn) of around 980 g mol^{-1} was purchased from Azevedo Industry and Trade of Oils Ltda (Itupeva, Sao Paulo, Brazil). Microcrystalline cellulose (MCC, Avicel PH 101) was donated by Valdequímica Chemical Products Ltda, São Paulo, Brazil. It was dried in an air-circulated oven at 105 °C for 4 h before use for the preparation of CNC and composites.

2.2. Preparation of Cellulose Nanocrystals

Cellulose nanocrystals (CNC) were extracted from MCC by acid hydrolysis using an aqueous solution of sulfuric acid (64% w/w), at a temperature of 44 °C for 130 min. The crude suspension was quenched with ice, exhaustively washed with distilled water, followed by centrifugation allowing the removal of the excess acid. The final purification was performed by dialysis against water for several days until the pH was equal to that of the starting water. The purified nanocrystals were suspended in water and sonicated for 30 min, followed by filtration on a glass filter. A few drops of chloroform were added to the nanocrystal suspension that was stored at 4 °C. Prior to use, the nanocrystals were obtained through the freeze-drying of the suspension.

2.3. Chemical Modification of Sodium Lignosulfonate with Glutaraldehyde (LS-Glu)

In a three-neck round bottom flask, sodium lignosulfonate, glutaraldehyde, and potassium hydroxide were added in 1:2:0.075 (w/w) ratios. The reaction mixture was mechanically stirred at room temperature for 40 min. After this period of time, the reaction temperature was raised to 70 °C, and the mixture was mechanically stirred for 2 h. The crude product was cooled to room temperature, then neutralized with concentrated hydrochloric acid, and finally water was eliminated under reduced pressure. The dark brown solid was used in the subsequent steps.

2.4. Synthesis of Lignopolyurethane Thermoset with Concurrent Preparation of Composites

Sodium lignosulfonate modified with glutaraldehyde (66.7 g) was mechanically mixed with castor oil (76.5 g) for 5 min at room temperature. CNC or MCC (30 wt%, relative to the total mass of reagents) were added to the blend, and the resulting mixture was mechanically stirred for 10 min at room temperature. MDI (66.7 g) was added, and the mixture was mechanically stirred for

an additional 10 min at room temperature. The ratio NCO/OH considered was 1.2. Molding was performed using a metal mold ($300 \times 140 \times 5$ mm^3) under temperature and pressure using the following cycle (temperature/time/pressure): 35 °C/30 min/0 Pa; 45 °C /60 min/2.4 MPa; 60 °C/45 min/3.3 MPa; 85 °C/45 min/3.8 MPa; 120 °C/45 min/3.8 MPa; 150 °C/45 min/3.8 MPa.

2.5. Methods

Scanning electron micrographs of CNCs were taken with a FEI Company, model Magellan 400 L scanning electron microscope with a field emission gun (FESEM) with an acceleration voltage of 5 kV. The aspect ratio (L/d) of the nanocrystals was obtained from FESEM images using the image processing software ImageJ. Three different FESEM images and 82 measurements were used to determine the length and the diameter of CNC. The percolation threshold (ϕ_{Fc}) of the nanocrystals was calculated using the following equation:

$$\phi_{RFc} = \frac{0.7}{(L/d)} \tag{1}$$

in which L is the length and d the diameter of CNC, respectively.

Flexural strength measurements were performed according to the ASTM D 790 technical standard using an INSTRON universal piece of equipment, model 5569. The flexural strength values reported correspond to a 5% deformation because there was no fracture of the samples during the test. The determined D/e (D = length of span, e = thickness of the composite) ratio was 16 and with the following dimensions: 127 mm length $\times$ 12.7 mm width $\times$ 3.2 mm thickness, and eight specimens of each composite were tested.

The Izod impact strength was evaluated according to the ASTM D256 technical standard using Izod impact CEAST Resil 25 equipment (Instron, Norwood, MA, USA). The tests were carried out at room temperature with an impact speed of 4 m s^{-1} and incident energy of 5.5 J. For the tests, twenty unnotched samples with 63.5 mm length $\times$ 12.7 mm width $\times$ 4.5 mm thickness were used.

Scanning electron microscopy (SEM) images were obtained using a Zeiss-Leica apparatus, model 440, with an electron acceleration of 20 kV. Fractured samples were covered with a thin layer of gold using a sputter-coating system prior to analysis.

A dynamic mechanical analysis (DMA) (New Castle, DE, USA). was carried out using a DMA thermal analyzer, model Q800 from TA Instruments operating with the Dual Cantilever clamp (flexural mode). The dimensions of the samples were 64 mm length $\times$ 12 mm width $\times$ 3.2 mm thickness. The equipment was calibrated with a metallic standard sample provided by the supplier. The experimental conditions of the tests were: oscillation amplitude of 20 μm, 1 Hz frequency, and heating rate of 2 °C min^{-1} from -130 to 200 °C.

3. Results and Discussion

The SEM micrograph of MCC (Figure 1a) shows that the fibrous structure was kept after the industrial-scale process that yielded the microcrystalline cellulose.

When considering the use of CNC as reinforcement in composites, the percolation threshold (ϕ_{Fc}) of the nanocrystals is a very important parameter. According to the literature, if the weight fraction of reinforcement used in the formulation of the composite is higher than the percolation threshold, the density of cellulose nanocrystals in the matrix is sufficient to allow the connection of the nanocrystals through hydrogen bonds to yield a continuous three-dimensional network in the composite. This phenomenon occurs when the composites are prepared by casting/evaporation, allowing a random and homogeneous dispersion of the nanofiller. When using melt processing, the orientation of the cellulosic nanorods limits their possible connection [32]. This 3D network, in turn, provides composite materials with superior mechanical properties. The morphology and dimensions of the CNC, i.e., their aspect ratio, determine the percolation threshold, as shown from Equation (1). Therefore, the percolation threshold depends on the cellulose source and conditions used to prepare the nanocrystals.
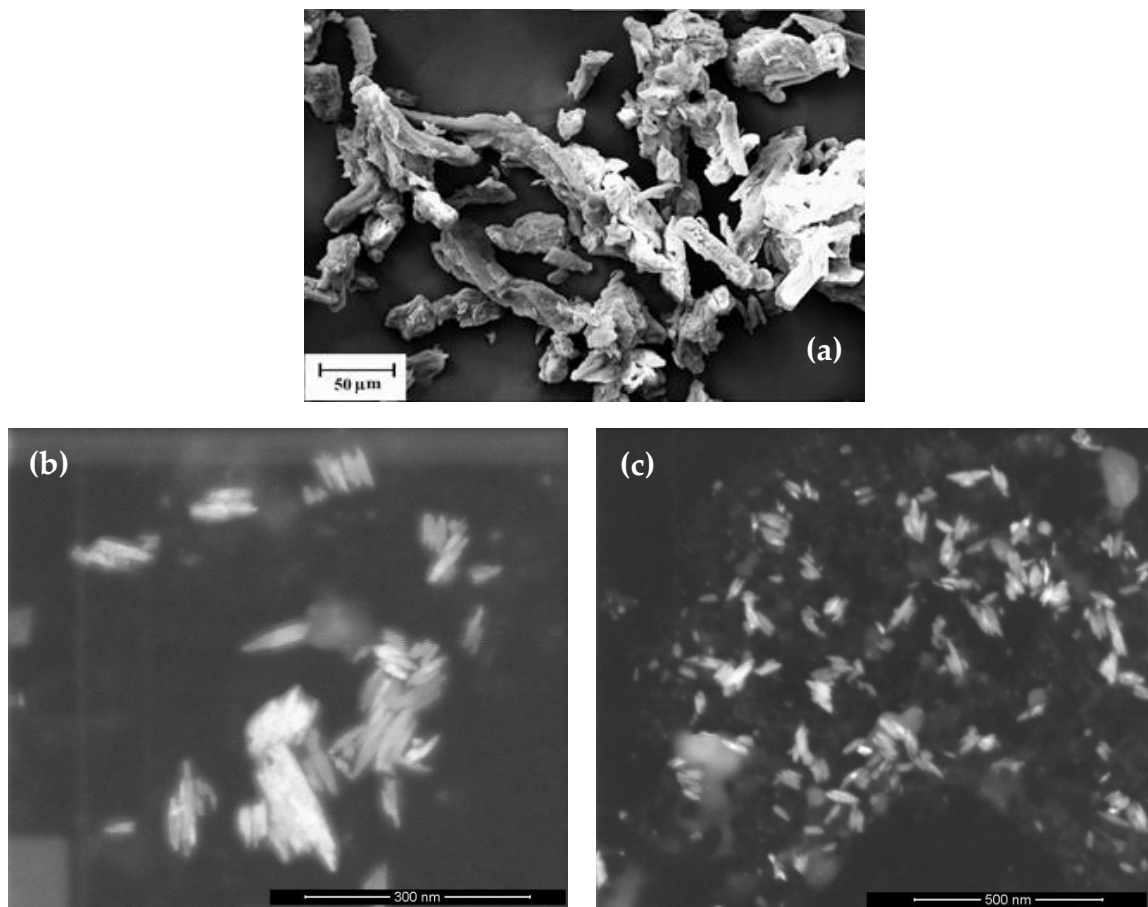
Figure 1. SEM images for (**a**) MCC and (**b**,**c**) CNC extracted from MCC by acid hydrolysis.

SEM images (Figure 1b,c) of the nanocrystals prepared in this work revealed a needle-like morphology, whose length and diameter were 91 ± 10 nm and 8 ± 1 nm, respectively. Therefore, the aspect ratio of the nanocrystals was about 11.4. Using Equation (1) (see Materials and Methods Section), the percolation threshold for the nanocrystals was about 6.2 vol%. Accordingly, our composites, which are reinforced with 30 wt% nanocrystals, were expected to form a percolating network of nanocrystals. Indeed, assuming a density of 1.6 and 1 g·cm^{-3} for crystalline cellulose and lignopolyurethane, respectively, 30 wt% CNC corresponds to 22.2 vol% CNC, i.e., well above the percolation threshold. The SEM images also showed the tendency of the nanocrystals to laterally aggregate. The observed aggregation phenomenon is most likely driven by hydrogen bonds between the nanocrystals, which are favored if the nanocrystals are freeze-dried as in the present study. It should be noted that freeze-drying of the cellulose nanocrystal suspension was mandatory as water would react with the isocyanate groups on MDI to yield 4,4'-methylenedianiline and carbon dioxide. Therefore, the classical use of an aqueous suspension of CNC in the preparation of the targeted composites would prevent the formation of the lignopolyurethane matrix.

The positive effect of both MCC and CNC on the mechanical properties of the composites can be observed from the results of the flexural tests reported in Table 1. The composite reinforced with CNC showed the highest flexural modulus among the materials investigated. Reinforcement with nanocrystals improved the flexural modulus of the lignopolyurethane matrix by approximately 670%, and an improvement of about 520% was observed for the composite reinforced with MCC, indicating that the CNC-reinforced composite resisted more to the deformation than the MCC reinforced composite. The flexural strength for both composites was higher than that of the pristine polymer, but considering the errors (MCC: ±0.9, CNC: ±0.5) both composites showed similar values (Table 1).

Table 1. Flexural modulus (at 5% deformation) (E_F), flexural strength (σ_F), and Izod (unnotched) impact strength (IS) for the pristine lignopolyurethane, lignopolyurethane reinforced with MCC, and lignopolyurethane reinforced with CNC.

Material	E_F (MPa)	σ_F (MPa)	IS (J/m)
Pristine lignopolyurethane	120 ± 30	4.0 ± 0.6	28 ± 3
MCC composite	620 ± 10	10.9 ± 0.9	46 ± 2
CNC composite	800 ± 50	10.3 ± 0.5	48 ± 5

It is worth noting that the flexural strength values reported in Table 1 correspond to values at 5% deformation, as the materials did not break during the test. The use of CO as a source of polyol in the synthesis of lignopolyurethanes, in addition to lignosulfonate, introduced flexible aliphatic segments in the chemical structure of the polymer. In the present study, this led to unbreakable materials when subjected to flexural stress, including the neat polymer and the composites reinforced with CNC and CMC.

Reinforcement with CNC or MCC also led to materials with higher impact strength properties (Table 1). An improvement of about 170% in impact strength was observed for the composites compared to the pristine lignopolyurethane, indicating the efficient load transfer from the matrix to the cellulosic phase. However, the nano and micro composites had virtually the same value for impact strength, showing that CNC and MCC exhibited the same capacity to dissipate the impact energy transferred from the matrix to the reinforcement through the interface.

The SEM image of the fractured surface of the pristine polymer shows the presence of pores and cavities (Figure 2a), which may have been generated by the reaction of isocyanate groups with residual water, which generates CO_2. For both composites reinforced with CNC (Figure 2b,c) and with MCC (Figure 2d,e), the presence of pores and cavities in the fractured surfaces decreased significantly compared to the neat polymer (Figure 2a).

The fracture surface does not show the presence of CNC aggregates (see Figure 1), indicating that the nanocrystals were covered by the matrix (Figure 2b,c). The fractured surface of the composite reinforced with MCC shows the short fibers of microcrystalline cellulose covered by the lignopolyurethane matrix (arrows in Figure 2e). The coverage of both CNC and MCC by the lignopolyurethane matrix was expected and favored by attractive interactions between polar groups, as well as between non-polar domains, from both the polymer and the reinforcement.

The evolution of the storage modulus (E') as a function of the temperature was investigated by DMA tests (Figure 3a). For pristine lignopolyurethane and at low temperature, E' slightly decreased with the temperature from about 1 GPa to 500 MPa. The polymer was in the glassy state, and molecular motions were largely restricted to vibration and short-range rotational motions. Adding CNC or MCC successively increased the value of E' to a few GPa. This increase in the modulus value even below the glass transition temperature is good evidence of the strong reinforcing tendency of both cellulosic fillers to the matrix. Around 25 °C, a sharp modulus drop appeared for all samples. It corresponds to the beginning of the temperature range at which the glass transition of the polymeric matrix occurs. This modulus drop was associated with an energy dissipation phenomenon evidenced in the concomitant relaxation process where the loss angle tangent (tan δ) passed through a maximum (Figure 3b).

This relaxation process involves cooperative motions of long-segments sequences. For higher temperatures, the modulus tended to stabilize (rubbery modulus). For pristine lignopolyurethane, the modulus slightly increased from about 125 °C. It is attributed to crosslinking reactions that occur during the temperature scan and make the polymer stiffer. No significant difference was observed between CNC- and MCC-reinforced composites.
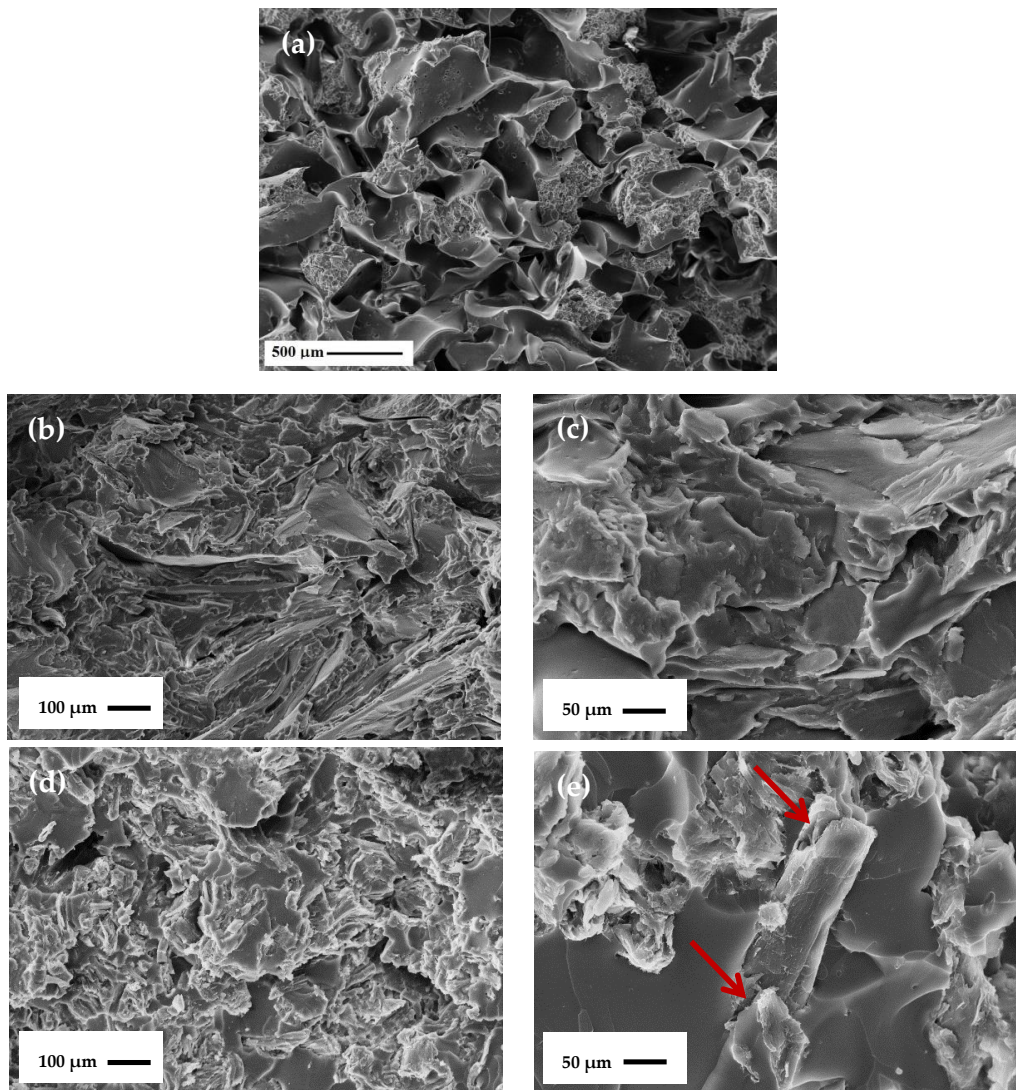
Figure 2. SEM images of the fractured surfaces for (**a**) pristine lignopolyurethane and composites reinforced with (**b**,**c**) CNC and (**d**,**e**) MCC; the arrows indicate the short MCC fibers covered by the matrix.
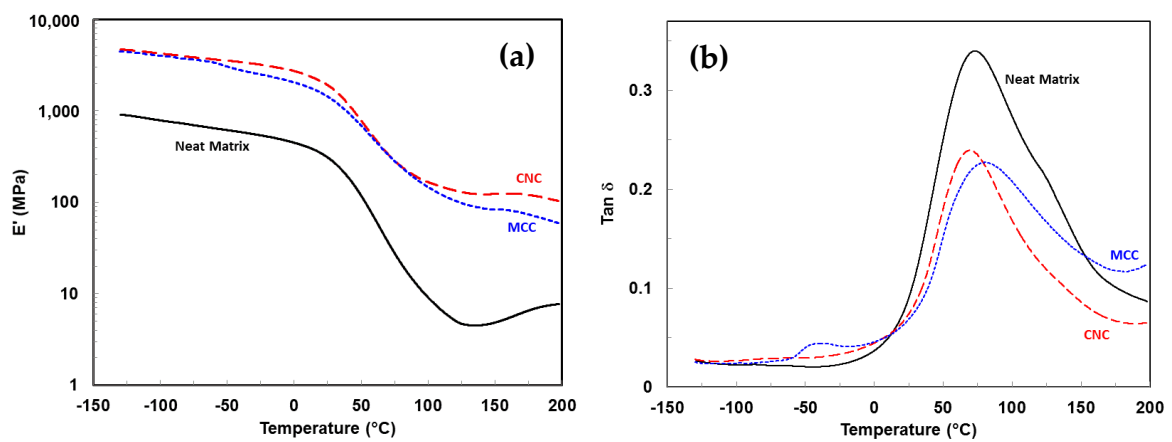

Figure 3. (**a**) Storage modulus (E′) and (**b**) loss angle tangent (tan δ) versus temperature for the neat lignopolyurethane and lignopolyurethane composites reinforced with cellulose nanocrystals (CNC) and microcrystalline cellulose (MCC).

The tan δ curves of the investigated materials (Figure 3b) revealed a peak around 70–80 °C. It is attributed to the main relaxation process associated with the glass transition (Tg) of the polymeric matrix. The tan δ value corresponds to the ratio of loss (E″) and storage (E′) moduli at the corresponding temperature, being an indicator of the damping property of the material, resulting from the balance between the loss and storage moduli. The presence of MCC or CNC increased the value of both E″ (curves not shown) and E′ (Figure 3a). The energy dissipation capacity (related to E″) increased less than the energy storage capacity (E′), compared to the neat polymer, which led to a decrease in the magnitude of the tan δ peak (Figure 3b). Interactions at a molecular level between the reinforcement and matrix decrease the mobility of the polymeric segments present at the interface, leading to less energy dissipation, thus decreasing the height of the tan δ peak. The peak height of the MCC composite was slightly smaller than that of the CNC composite, and additionally we noted a shift of the peak to a slightly higher temperature, which can be taken as an indication of less mobility of the lignopolyurethane segments at the interface for the MCC composite. In the transition to the rubbery state, after Tg, the MCC composite had slightly lower values of E′ than the CNC composite (Figure 3a), which led to higher tan δ values for the MCC composite at higher temperatures. The broader peak width of this composite can be attributed to less homogeneity in the distribution of MCC in the matrix, compared to CNC (Figure 3b).

We tried to predict the evolution of the storage modulus for CNC-reinforced composites using two theoretical models. The first one is based on a mean-field approach (Halpin-Kardos model) and the second one on the percolation approach. These two approaches are classically used for this kind of material, and details of the calculation can be found elsewhere [33]. The main equations used are reported in Appendices A and B for the mean-field and percolation approaches, respectively. For the formed approach (Halpin-Kardos), the prediction of the modulus of the composite is governed by the size, shape, and volume fraction of the filler, and also by the mechanical properties of both the matrix and the fibers, taking into account the mechanical anisotropy of CNC. The Poisson's ratio of the matrix (ν_M) was set at 0.3 and 0.5 in the glassy and rubbery states, respectively, and the Poisson's ratio of crystalline cellulose (ν_F) was set at 0.3. The modulus of CNC in the longitudinal (E_{11F}) and transverse directions (E_{22F}) was assumed to be 130 GPa [34] and 15 GPa [35], respectively, and the in-plane shear modulus of CNC (G_F) was valued at 5 GPa [35]. The modulus of the polymeric matrix was determined from experimental DMA measurements. For the percolation prediction, the critical percolation exponent (b) was set at 0.4 [33]. The modulus of the percolating CNC network (E_R) is more elusive. It obviously depends on the interactions between CNC and can be determined by performing tensile tests on films obtained by the water evaporation of CNC suspensions, but also on CNC–matrix interactions that can disturb CNC–CNC interactions in the composite. A correlation was found between the stiffness of CNC films and the aspect ratio of the constituent rod-like nanoparticles [36]. The aspect ratio of CNC extracted from MCC (11.4) is close to the one observed for CNC derived from sugar cane bagasse (12.9), ramie fibers (12.4), and cotton (11.3), for which the CNC film modulus was found to be 1.50, 0.46, and 2.13 GPa, respectively [36]. The percolation prediction was therefore carried out using two E_R modulus values, i.e., 2 and 0.5 GPa.

Figure 4 shows the comparison between the experimental storage modulus data obtained for the lignopolyurethane composite reinforced with CNC and the prediction from the Halpin-Kardos and percolation approaches. It appears that the Halpin-Kardos model gives a much better description of the experimental behavior in the glassy state of the matrix whereas it strongly underestimates the rubbery modulus. A better prediction of the experimental modulus of the lignopolyurethane composite reinforced with CNC is obtained from the percolation approach, and it clearly appears that the modulus of the percolating CNC network is between 500 MPa and 2 GPa.
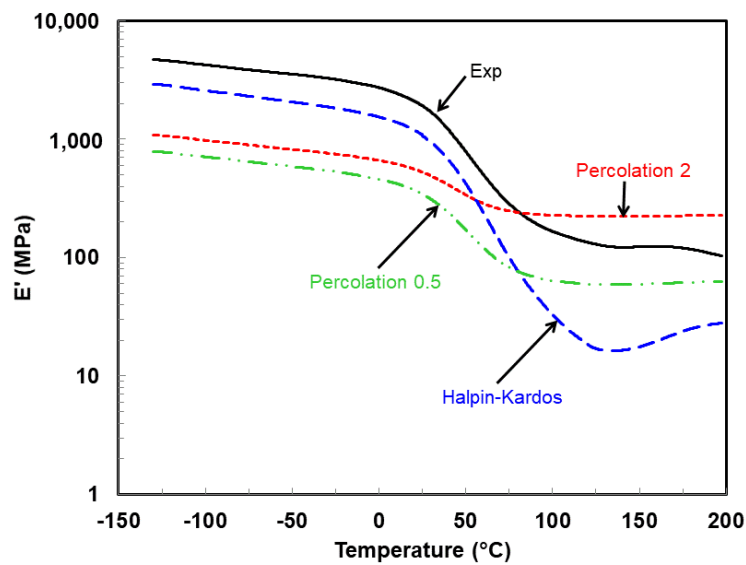
Figure 4. Storage modulus (E′) versus temperature for the lignopolyurethane composite reinforced with CNC. Comparison between the experimental data (Exp) and predicted data from the Halpin-Kardos model (Halpin-Kardos), and percolation approach using a modulus of 0.5 GPa (Percolation 0.5) or 2 GPa (Percolation 2) for the percolating CNC network (E_R).

4. Conclusions

Sodium lignosulfonate and castor oil were successfully employed in the preparation of a polyurethane matrix, which was used for preparing composites reinforced with CNC or MCC. The set of results obtained showed that CNC and MCC are promising reinforcements for polyurethane-type matrices and can be used interchangeably because, in general, both composites exhibited similar properties. The CNC composite showed superiority to the MCC one regarding the flexural modulus, indicating the first as being the material of choice when the resistance to flexural deformation is critical. The results highlight the use of MCC in composites, given the wide availability of this material around the world. The composites reported herein were chiefly composed of renewable raw materials, thereby meeting the current expectations concerning sustainability.

Appendix A

The modulus (E) of the composite predicted by the mean-field approach (Halpin-Kardos model) is given by Equation (A1):

$$E = \frac{4U_2(U_1 - U_2)}{U_1} \tag{A1}$$

where

$$U_1 = \frac{1}{8}(3Q_{11} + 3Q_{22} + 2Q_{12} + 4Q_{66}) \tag{A2}$$

$$U_2 = \frac{1}{8}(Q_{11} + Q_{22} - 2Q_{12} + 4Q_{66}) \tag{A3}$$

with

$$Q_{ii} = \frac{E_{ii}}{1 -_{12} \times v_{21}}(i = 1, \, 2) \tag{A4}$$

$$Q_{12} =_{12} \times Q_{22} = v_{21} \times Q_{11} \tag{A5}$$

$$Q_{66} = G_{12} \tag{A6}$$

where E_{11}, E_{22}, and G_{12} are the modulus of the composite in the fiber direction, modulus of the composite perpendicular to the fiber direction, and in-plane shear modulus of the composite, respectively, which are given by the following equations:

$$\frac{E_{ii}}{E_M} = \frac{(1 + \xi_{ii}\phi_F)E_{iiF} + \xi_{ii}(1 - \phi_F)E_M}{(1 - \phi_F)E_{iiF} + (\xi_{ii} + \phi_F)E_M}(i = 1, \, 2) \tag{A7}$$

$$\frac{G_{12}}{G_M} = \frac{(1 + \phi_F)G_F + (1 - \phi_F)G_M}{(1 - \phi_F)G_F + (1 + \phi_F)G_M} \tag{A8}$$

The Poisson's ratio v_{12} can be estimated by a mixing rule:

$$v_{12} = v_M\phi_M + v_F\phi_F = \frac{Q_{11}}{Q_{22}} \times v_{21} = \frac{E_{11}}{E_{22}} \times v_{21} \tag{A9}$$

The Poisson' ratio of the polymer matrix (v_M) was set at 0.3 and 0.5 in the glassy and rubbery states, respectively, and the Poisson' ratio of cellulose (v_F) was set at 0.3. The volume fraction of cellulose (φ_F) is 22.2 vol%, and the volume fraction of the matrix (φ_M) is 77.8 vol%.

The ξ_{ii} parameters are related to the length (L) and diameter (d) of the fibers:

$$\xi_{11} = 2 \times \frac{L}{d} \text{and} \xi_{22} = 2 \tag{A10}$$

E_{11F}, E_{22F}, and G_F correspond to the longitudinal, transverse, and shear modulus of CNC estimated as 130 GPa, 15 GPa, and 5 GPa, respectively. E_M is the tensile modulus of the polymer matrix, which is determined experimentally and whose value changes with the temperature, and G_M is the shear modulus of the polymer matrix given by $G_M = 2(1 + v_M)E_M$.

Appendix B

The modulus (E) of the composite predicted by the percolation approach is given by Equation (A11):

$$E = \frac{(1 - 2\psi + \psi\phi_F)E_M E_R + (1 - \phi_F)\psi E_R^2}{(1 - \phi_F)E_R + (\phi_F - \psi)E_M} \tag{A11}$$

where E_R corresponds to the modulus of the percolating CNC network, which was set at 0.5 and 2 GPa, and ψ is the volume fraction of the percolating CNC network given by:

$$\psi = \phi_F\left(\frac{\phi_F - \phi_{Fc}}{1 - \phi_{Fc}}\right)^b \tag{A12}$$

The critical exponent b was set at 0.4.

References

1.　Yu, J.; Ai, F.; Dufresne, A.; Gao, S.; Huang, J.; Chang, P.R. Structure and mechanical properties of poly(lactic acid) filled with (starch nanocrystals)-graft-poly(ε-caprolactone). *Macromol. Mater. Eng.* **2008**, *293*, 763–770. [CrossRef]

2. Lin, N.; Chen, G.; Huang, J.; Dufresne, A.; Chang, P.R. Effects of polymer-grafted natural nanocrystals on the structure and mechanical properties of poly(lactic acid): A case of cellulose whisker-graft-polycaprolactone. *J. Appl. Polym. Sci.* **2009**, *113*, 3417–3425. [CrossRef]

3. Feng, L.; Zhou, Z.; Dufresne, A.; Huang, J.; Wei, M.; An, L. Structure and properties of new thermoforming bionanocomposites based on chitin whiskers-graft-polycaprolactone. *J. Appl. Polym. Sci.* **2009**, *112*, 2830–2837. [CrossRef]

4. Chen, G.; Dufresne, A.; Huang, J.; Chang, P.R. A novel thermoformable bionanocomposite based on cellulose nanocrystal-graft-poly(ε-caprolactone). *Macromol. Mater. Eng.* **2009**, *294*, 59–67. [CrossRef]

5. Gao, Z.; Peng, J.; Zhong, T.; Sun, J.; Wang, X.; Yue, C. Biocompatible elastomer of waterborne polyurethane based on castor oil and polyethylene glycol with cellulose nanocrystals. *Carbohydr. Polym.* **2012**, *87*, 2068–2075. [CrossRef]

6. Siqueira, G.; Bras, J.; Dufresne, A. Cellulose whiskers versus microfibrils: Influence of the nature of the nanoparticle and its surface functionalization on the thermal and mechanical properties of nanocomposites. *Biomacromolecules* **2009**, *10*, 425–432. [CrossRef]

7. Habibi, Y.; Goffin, A.L.; Schiltz, N.; Duquesne, E.; Dubois, P.; Dufresne, A. Bionanocomposites based on poly(ε-caprolactone)-grafted cellulose nanocrystals by ring-opening polymerization. *J. Mater. Chem.* **2008**, *18*, 5002–5010. [CrossRef]

8. Klemm, D.; Heublein, B.; Fink, H.P.; Bohn, A. Cellulose: Fascinating biopolymer and sustainable raw material. *Angew. Chem. Int. Ed.* **2005**, *44*, 3358–3393. [CrossRef]

9. Jiang, F.; Hsieh, Y.L. Chemically and mechanically isolated nanocellulose and their self-assembled structures. *Carbohydr. Polym.* **2013**, *95*, 32–40. [CrossRef]

10. Ramires, E.C.; Dufresne, A. A review of cellulose nanocrystals and nanocomposites. *TAPPI J.* **2011**, *10*, 9–16. [CrossRef]

11. Ramires, E.C.; Dufresne, A. Cellulose nanoparticles as reinforcement in polymer nanocomposites. In *Advances in polymer nanocomposites: Types and Applications*; Gao, F., Ed.; Woodhead Publishing: Cambridge, UK, 2012; pp. 131–163. [CrossRef]

12. Ranby, B.G. Fibrous macromolecular systems. Cellulose and muscle. The colloidal properties of cellulose micelles. *Discuss. Faraday Soc.* **1951**, *11*, 158–164. [CrossRef]

13. Battista, O.A.; Coppick, S.; Howsmon, J.A.; Morehead, F.F.; Sisson, W.A. Level-off degree of polymerization: Relation to polyphase structure of cellulose fibers. *Ind. Eng. Chem.* **1956**, *48*, 333–335. [CrossRef]

14. Hamad, W.Y.; Hu, T.Q. Structure-process-yield interrelations in nanocrystalline cellulose extraction. *Can. J. Chem. Eng.* **2010**, *88*, 392–402. [CrossRef]

15. Bondeson, D.; Mathew, A.; Oksman, K. Optimization of the isolation of nanocrystals from microcrystalline cellulose by acid hydrolysis. *Cellulose* **2006**, *13*, 171–180. [CrossRef]

16. Dufresne, A. Polysaccharide nano crystal reinforced nanocomposites. *Can. J. Chem.* **2008**, *86*, 484–494. [CrossRef]

17. Bitinis, N.; Verdejo, R.; Bras, J.; Fortunati, E.; Kenny, J.M.; Torre, L.; López-Machado, M.A. Poly(lactic acid)/natural rubber/cellulose nanocrystal bionanocomposites Part I. Processing and morphology. *Carbohydr. Polym.* **2013**, *96*, 611–620. [CrossRef]

18. Fortunati, E.; Puglia, D.; Luzi, F.; Santulli, C.; Kenny, J.M.; Torre, L. Binary PVA bio-nanocomposites containing cellulose nanocrystals extracted from different natural sources: Part I. *Carbohydr. Polym.* **2013**, *97*, 825–836. [CrossRef]

19. Garba, Z.N.; Zhou, W.; Lawan, I.; Zhang, M.; Yuan, Z. Enhanced removal of prometryn using copper modified microcrystalline cellulose (Cu-MCC): Optimization, isotherm, kinetics and regeneration studies. *Cellulose* **2019**, *26*, 6241–6258. [CrossRef]

20. Trache, D.M.; Hussin, H.; Hui Chuin, C.T.; Sabar, S.; Fazita, M.R.N.; Taiwo, O.F.A.; Hassan, T.M.; Haafiz, M.K.M. Microcrystalline cellulose: Isolation, characterization and bio-composites application-a review. *Int. J. Biol. Macromol.* **2016**, *93*, 789–804. [CrossRef]

21. Zhang, Q.; Lei, H.; Cai, H.; Han, X.; Lin, X.; Qian, M.; Zhao, Y.; Huo, E.; Villota, E.M.; Mateo, W. Improvement on the properties of microcrystalline cellulose/polylactic acid composites by using activated biochar. *J. Clean. Prod.* **2020**, *252*, 119898. [CrossRef]

22.	Bhasney, S.M.; Kumar, A.; Katiyar, V. Microcrystalline cellulose, polylactic acid and polypropylene biocomposites and its morphological, mechanical, thermal and rheological properties. *Compos. B Eng.* **2020**, *184*, 107717. [CrossRef]

23.	Medronho, B.; Lindman, B. Brief overview on cellulose dissolution/regeneration interactions and mechanisms. *Adv. Colloid Interface Sci.* **2015**, *222*, 502–508. [CrossRef] [PubMed]

24.	Kostov, K.G.; Dos Santos, A.L.R.; Nascente, P.A.P.; Kayama, M.E.; Mota, R.P.; Algatti, M.A. Surface modification of siloxane containing polyurethane polymer by dielectric barrier discharge at atmospheric pressure. *J. Appl. Polym. Sci.* **2012**, *125*, 4121–4127. [CrossRef]

25.	Krasowska, K.; Janik, H.; Gradys, A.; Rutkowska, M. Degradation of polyurethane in compost under natural conditions. *J. Appl. Polym. Sci.* **2012**, *125*, 4252–4260. [CrossRef]

26.	Cassales, A.; Ramos, L.A.; Frollini, E. Synthesis of bio-based polyurethanes from Kraft lignin and castor oil, with simultaneous film formation. *Int. J. Biol. Macromol.* **2020**, *145*, 28–41. [CrossRef]

27.	Cateto, C.A.; Barreiro, M.F.; Rodrigues, A.E.; Belgacem, M.N. Kinetic study of the formation of lignin-based polyurethanes in bulk. *React. Func. Polym.* **2011**, *71*, 863–869. [CrossRef]

28.	Ramires, E.C.; Oliveira, F.; Frollini, E. Composites based on renewable materials: Polyurethane-type matrices from forest byproduct/vegetable oil and reinforced with lignocellulosic fibers. *J. Appl. Polym. Sci.* **2013**, *129*, 2224–2233. [CrossRef]

29.	Hatakeyama, T.; Matsumoto, Y.; Asano, Y.; Hatakeyama, H. Glass transition of rigid polyurethane foams derived from sodium lignosulfonate mixed with diethylene, triethylene and polyethylene glycols. *Thermochim. Acta* **2004**, *416*, 29–33. [CrossRef]

30.	Da Silva, C.G.; Grelier, S.; Pichavant, F.; Frollini, E.; Castellan, A.; Frollini, E.; Castellan, A. Adding value to lignins isolated from sugarcane bagasse and Miscanthus. *Ind. Crops Prod.* **2013**, *42*, 87–95. [CrossRef]

31.	Oliveira, F.D.; Ramires, E.C.; Frollini, E.; Belgacem, M.N. Lignopolyurethanic materials based on oxypropylated sodium lignosulfonate and castor oil blends. *Ind. Crops Prod.* **2015**, *72*, 77–86. [CrossRef]

32.	Mariano, M.; El Kissi, N.; Dufresne, A. Structural reorganization of CNC in injection-molded CNC/PBAT materials under thermal annealing. *Langmuir* **2016**, *32*, 10093–10103. [CrossRef] [PubMed]

33.	Dufresne, A. *Nanocellulose: From Nature to High Performance Tailored Materials*, 2nd ed.; Walter de Gruyter GmbH & Co KG: Berlin, Germany, 2017.

34.	Dufresne, A. Cellulose nanomaterial reinforced polymer nanocomposites. *Curr. Opin. Colloid Interface Sci.* **2017**, *29*, 1–8. [CrossRef]

35.	Favier, V.; Canova, G.R.; Cavaillé, J.Y.; Chanzy, H.; Dufresne, A.; Gauthier, C. Nanocomposites materials from latex and cellulose whiskers. *Polym. Advan. Technol.* **1995**, *6*, 351–355. [CrossRef]

36.	Bras, J.; Viet, D.; Bruzzese, C.; Dufresne, A. Correlation between stiffness of sheets prepared from cellulose whiskers and nanoparticles dimensions. *Carbohydr. Polym.* **2011**, *84*, 211–215. [CrossRef]